Journal of Inorganic Biochemistry 158 (2016) 11–16

Contents lists available at ScienceDirect

Journal of Inorganic Biochemistry

journal homepage: www.elsevier.com/locate/jinorgbio

Mixed regiospecificity compromises alkene synthesis by a cytochrome P450 peroxygenase from *Methylobacterium populi*

Jose A. Amaya, Cooper D. Rutland, Thomas M. Makris *

University of South Carolina, Department of Chemistry and Biochemistry, 631 Sumter Street, Columbia, SC 29208, United States

ARTICLE INFO

Article history:
Received 25 October 2015
Received in revised form 1 February 2016
Accepted 25 February 2016
Available online 27 February 2016

Keywords:
Cytochrome P450
Monooxygenase
Oxygen activation
Oxidative decarboxylation
Hydrocarbon biosynthesis

ABSTRACT

Intensive interest has focused on enzymes that are capable of synthesizing hydrocarbons, alkenes and alkanes, for sustainable fuel production. A recently described cytochrome P450 ($OleT_{JE}$) from the CYP152 family catalyzes an unusual carbon–carbon scission reaction, transforming C_n fatty acids to C_{n-1} 1-alkenes. Here, we show that a second CYP152, CYP-MP from *Methylobacterium populi* ATCC BAA 705, also catalyzes oxidative substrate decarboxylation. Alkene production is accompanied with the production of fatty alcohol products, underscoring the mechanistic similarity of the decarboxylation reaction with canonical P450 monooxygenation chemistry. The branchpoint of these two chemistries, and regiospecificity of oxidation products, is strongly chain length dependent, suggesting an importance of substrate coordination for regulating alkene production.

1. Introduction

Widespread biotechnological interest has focused on the identification [1–4] and reconstitution of enzymes capable of synthesizing gaseous [5,6] or liquid hydrocarbon fuels in microbial hosts [5,7–9]. A recently discovered cytochrome P450 isolated from *Jeotgalicoccus* sp. ATCC 8456, termed $OleT_{JE}$ [2] (or CYP152L1) [10], catalyzes the hydrogen peroxide dependent cleavage of C_n fatty acids for the synthesis of C_{n-1} alkenes and a carbon dioxide co-product [11]. The OleT reaction converts a biologically abundant feedstock into a hydrocarbon (and useful commodity chemical for organic synthesis) in a one-step reaction that consumes an inexpensive co-substrate. Given its tremendous potential for advanced biofuel production, a number of recent efforts have focused on the optimization of OleT catalysis. These include the development of alternative photo- [12] and bio- [13,14] catalytic turnover methods to maximize alkene production in vitro, thereby potentially bypassing the requirement for H_2O_2, which may prove to be more difficult to leverage in a microbial platform.

The oxidative decarboxylation reaction catalyzed by OleT is highly atypical, although not unprecedented [15,16], for P450s, which typically catalyze the monooxygenation of substrates (reviewed in [17,18]). Primary sequence analysis places OleT as a member of the CYP152 family, which includes the fatty acid hydroxylases P450 SPα [19–22], P450 BSβ [23] and P450 CLA [24]. The structure of OleT, solved by the Munro and Leys groups, has confirmed a high degree of structural similarity of the OleT active-site [10] with BSβ [23]and SPα [25], including direct interaction of the fatty acid carboxylate necessary for the efficient utilization of H_2O_2 with an active site arginine (Arg245 in OleT). A large steady-state substrate 2H kinetic isotope effect (KIE) [26] for SPα and BSβ hydroxylations indicates that the peroxygenase reaction proceeds by substrate C–H bond abstraction by a high-valent iron(IV)-oxo π cation radical Compound I intermediate [27]. Ensuing oxygen rebound [28,29] results in a distribution of α and β mono-hydroxylated products.

In recent work by our laboratory [11], we evaluated the mechanism of the OleT alkene forming reaction with an eicosanoic (C_{20}) fatty acid substrate, a chain length which is presumed to approximate the native substrate of OleT based on identification of 18-methyl-nonadecene as the predominant alkene found in *Jeotgalicoccus* [2]. Substrate and H_2O_2 labeling studies confirmed that alkene formation is accompanied with the formation of a carbon dioxide co-product that derives from the fatty acid terminal carboxylate. Significantly, no oxygen insertion was observed in the CO_2 co-product, hinting at a clear mechanistic deviation of alkene forming and P450 monooxygenation chemistries. Further evaluation of the OleT reaction by single-turnover stopped flow kinetics, however, strongly links the two mechanisms [11]. Rapid mixing of per-deuterated C_{20} fatty acid bound with H_2O_2 resulted in the direct observation of a catalytically competent Compound I species [27,30,31] on route to alkene formation. This species did not significantly accumulate in parallel reactions with protiated substrate, suggesting that alkene formation also proceeds by substrate hydrogen atom abstraction. Taken together, the mechanisms for P450 aliphatic

Abbreviations: TEV, tobacco etch virus endopeptidase; GST, glutathione S transferase; EPR, electron paramagnetic resonance; LS, low-spin heme iron; HS, high-spin heme iron; BSTFA, N,O-Bis(trimethylsilyl)trifluoroacetamide; CL, chain length; KIE, Kinetic Isotope Effect.

* Corresponding author.
E-mail address: makrist@mailbox.sc.edu (T.M. Makris).

http://dx.doi.org/10.1016/j.jinorgbio.2016.02.031
0162-0134/

hydroxylations, and the initial steps for OleT oxidative decarboxylation, provides evidence for branching following an initial C–H bond abstraction event, as depicted in Fig. 1. This scheme is additionally supported by altered product profiles observed for OleT in reactions with shorter fatty acid substrates. Although OleT predominantly generates 1-nonadecene in single [11] and multiple turnover [2,13] reactions with eicosanoic acid (C_{20}), the metabolism of shorter chain length substrates often results in an increased production of hydroxylated fatty acid side products [13,32].

Important questions remain regarding the relative importance of electronic and active-site structural contributions on the hydroxylation/decarboxylation branchpoint in OleT, which would potentially aid in leveraging its catalysis further. This has prompted us to reexamine the efficiency of alkene production by CYP152 orthologs. While OleT is the founding member for P450 fatty acid decarboxylases, work by Rude et al. previously demonstrated that other CYP152 enzymes may also have the capacity to produce alkenes [2]. Among a series of CYP152 enzymes tested towards palmitic acid (C_{16}) decarboxylation in that study, a P450 from *Methylobacterium populi* ATCC BAA 705 (accession number ZP_02200540), which we denote hereafter as CYP-MP, was found to produce pentadecene. The reported high chemoselectivity of CYP-MP towards palmitic acid decarboxylation, and low sequence identity of CYP-MP to OleT (31%), including significant differences in active-site, made it an attractive system to begin to evaluate structural contributions on alkene formation. Here, we have cloned, overexpressed, and characterized CYP-MP reactivity towards a panel of fatty acid chain length substrates. Analytical experiments provide evidence for low alkene yields, and a large distribution of hydroxylation products that surprisingly extends beyond the fatty acid Cβ position. Product yield, efficiency of alkene formation, and the regioselectivity of products show significant chain length dependence. We have additionally examined the proposed role of an active-site histidine in OleT, thought to be important for alkene production, through its introduction into CYP-MP.

2. Experimental procedures

2.1. Reagents

Ni-NTA and Butyl Sepharose resins were obtained from Qiagen and GE Healthcare respectively. An *Escherichia coli* codon optimized gene of Mpop_1292, the orf encoding CYP-MP from *M. populi* (ATCC BAA-705) was synthesized by DNA2.0 (Menlo Park, CA). The original construct contained a C-terminal TEV cleavage site followed by a His_6 tag. Fatty acids and N,O-Bis (trimethylsilyl) trifluoroacetamide (BSTFA) were purchased from the Supelco Analytical branch of Sigma Aldrich. Hydrogen peroxide was obtained from Sigma Aldrich. The pDB-HisGST and pMHTDelta238 (expressing tobacco etch virus (TEV) protease [33]) plasmids were obtained from the DNASU plasmid repository. Expression and purification of TEV followed described protocols [33].

2.2. Subcloning, heterologous expression and purification of Mpop_1292

The original CYP-MP expression plasmid was digested using NdeI and XhoI, excising the Mp_1292 gene, and ligated into a similarly digested pDB-HisGST. Cloning was verified by sequencing at ACGT Inc. Heterologous expression was performed in *E. coli* BL21 (DE3) cells using modified Terrific broth (consisting of 12 g. yeast extract, 6 g. tryptone and 1 g. bactopeptone, 125 mg thiamine, trace metals and 50 mg kanamycin per liter of culture). Cells were grown at 37 °C at 220 rpm, and the temperature was reduced to 20 °C at OD_{600} ~ 0.4 and supplemented with 10 mg/L delta aminolevulinic acid. At an OD_{600} ~ 1, cultures were induced with 0.1 mM IPTG. Cells were harvested after 24 h, centrifuged and stored at −80 °C. Preliminary expression trials indicated that the P450 was exclusively localized in the membrane fraction. As a result, the pellet was resuspended in lysis buffer containing detergent (50 mM potassium phosphate (KPi) pH 8, 10 mM imidazole, and 0.1 M NaCl, containing 0.8% w/v cholate, 1 mM PMSF and 15% (v/v) glycerol) (buffer A), and stirred for 2 h at 4 °C. Cells were disrupted using a Branson sonifier and allowed to stir for an additional hour. Following centrifugation for 45 min at 17,000g, the supernatant was loaded onto a Ni-NTA column, washed with 10 column volumes of buffer A containing 30 mM imidazole, and eluted with buffer A with 250 mM imidazole. Cleavage of the N-terminal GST tag was performed by addition of 1 mg of TEV protease per 25 mg of P450 and proteolysis was allowed to proceed for 16 h at 4 °C. Ammonium sulfate was subsequently added to 25% saturation and the protein was loaded onto a butyl sepharose column equilibrated in 50 mM KPi pH 8, 0.1 M NaCl, 25% ammonium sulfate, and 15% glycerol (buffer B). The column was washed with 5 column volumes of buffer B and eluted with 50 mM KPi pH 8, 0.4% cholate and 15% glycerol. SDS-PAGE confirmed that the GST leader had been completely removed and that the protein was highly homogeneous. The final yield of purified P450 was roughly 40 mg per liter of culture.

2.3. Spectroscopy

Optical spectroscopy was performed on an Agilent 8453 spectrophotometer. An extinction coefficient of CYP-MP ($\varepsilon = 104\ mM^{-1}\ cm^{-1}$ at 422 nm) was determined using the pyridine hemochromagen method [34]. The ferrous carbonmonoxy P450 adducts were prepared by the addition of carbon monoxide gas to a solution of ferric P450, and subsequent reduction of the protein with sodium dithionite. EPR spectra were recorded using an X band Bruker EMXplus spectrometer equipped

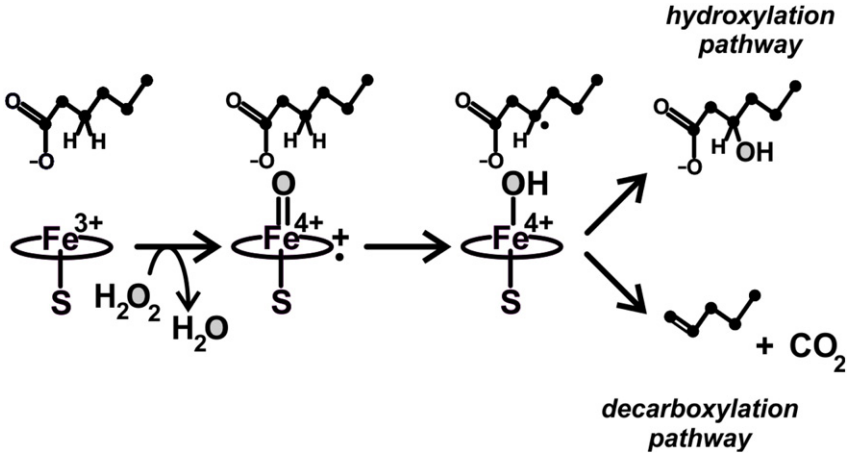

Fig. 1. Proposed mechanistic branching for fatty acid hydroxylation and decarboxylation catalyzed by OleT.

with an Oxford Instruments ESR900 liquid helium continuous flow cryostat. Spectra were recorded at a temperature of 20 K, a 1 mT modulation amplitude, and 1 mW microwave power. The concentration of protein was 200 μM.

2.4. Site directed mutagenesis

Site directed mutagenesis of the Mpop_M96H variant was performed using the following primer and its reverse complement: 5′ GATCATGGTTCTGTGCATGTTCTGGATGGTGCC 3′. Mutation was confirmed by gene sequencing at EtonBio Inc.

2.5. Optimizing turnover yields in OleT

OleT was expressed, purified, and adventitiously bound *E. coli* derived fatty acids were removed as described [11]. The effect of the rate of hydrogen peroxide addition on turnover efficiency was analyzed by mixing 2 mL of 5 mM hydrogen peroxide to a 2 mL reaction containing 200 mM KPi pH 7.5, 5 μM OleT and 500 μM eicosanoic acid (prepared as a 10 mM stock solution in DMSO). H_2O_2 was added either by fast addition or by calibrated delivery over the course of 30, 60 or 120 min using a New Era NE-1000 syringe pump. The reactions were quenched with 6 M HCl after 2 h (including addition time) and products were analyzed on gas chromatography as described in more detail below.

2.6. CYP-MP activity assays

Hydrogen peroxide (2 mL, 5 mM) was slowly added over the course of 1 h to a 2 mL reaction containing 200 mM KPi pH 7.5, 5 μM CYP-MP and 500 μM fatty acid (prepared as a 10 mM stock in DMSO) using a New Era NE-1000 syringe pump. Products were extracted by adding an equal volume of chloroform to the resulting reaction mixture. In order to account for differential response factors of alkenes, fatty acids and OH-fatty acids for accurate product quantitation, two internal standards (500 nmol of each) were added upon reaction completion. These consisted of 1-hexadecene throughout and a fatty acid two carbons shorter than the substrate. Following extraction, the organic phase was derivatized by adding 250 M equivalents of BSTFA (to initial substrate concentration) and incubated for 20 min at 60 °C. The derivatization mixture was dried using a stream of N_2 and redissolved in 100 μL $CHCl_3$. For gas chromatography (GC), 3 μL was analyzed on an Hewlett-Packard 5890 gas chromatograph using an HP-5 column with the following oven conditions: 170 °C for 3 min, a 10 °C/min to 220 °C, a 5 °C/min to 320 °C, and 320 °C for 3 min. The response factors between fatty acids, hydroxy fatty acids and alkenes were determined by analyzing known authentic fatty acids (C20–C10), 2-hydroxyhexadecanoic acid and 1-hexadecene standards.

2.7. GC mass spectrometry (GC–MS)

Gas chromatography mass spectrometry (GC–MS) was performed at the University of South Carolina Mass Spectrometry facility with a Hewlett Packard HP5890 GC and a 30 m Rbx-5 column. Mass spectra were recorded on a Waters VG 705 magnetic sector mass spectrometer using 70 eV electron impact energy.

3. Results

3.1. Heterologous expression and membrane localization of CYP-MP

A C-terminal hexahistidine tagged CYP-MP synthetic gene, behind a T5 promoter, showed poor expression in *E. coli* BL21(DE3), which did not improve upon alteration with a T7 promoter. In order to maximize expression, a TEV cleavable glutathione-S-transferase (GST) solubility tag was introduced at the N-terminus of CYP-MP by subcloning into the pDB-HisGST vector. Expression trials indicated a high level of protein production, and that the fusion was contained in the membrane fraction. In order to confirm subcellular localization, a membrane fraction was prepared by isolating spheroplasts, which were shown to contain at least 90% of CYP-MP (Fig. S1). Treatment of spheroplasts with detergent (0.8% sodium cholate) led to efficient solubilization of the fusion protein, which could be subsequently purified by affinity chromatography in the presence of detergent. The GST tag was cleaved as described in 2.2, and CYP-MP was purified from the GST fragment using hydrophobic interaction chromatography (Fig. S2). Native, untagged CYP-MP, which has a high predicted pI (~9.6), was found to require the presence of detergent in order to remain in a soluble, non-aggregated form. This feature suggests that the membrane localization of the full-length construct is likely not attributable to the presence of the N-terminal GST, but rather a general feature of CYP-MP.

3.2. Spectroscopic characterization of CYP-MP

The optical spectrum of untagged, cholate solubilized CYP-MP at pH 8.0 is shown in Fig. 1A and the inset. The purified ferric form of CYP-MP (solid line) has a perturbed red shifted Soret maximum at 422 nm, versus 417 nm that is typical for low-spin (LS) water bound P450s, a prominent α band at 545 nm and a significantly weaker β band at 575 nm. Significant hyperporphyrin characteristics [35] are also visible at ~360 nm. These spectroscopic features are indicative of an altered coordination environment in CYP-MP, possibly deriving from binding of an alternative axial ligand [36] [37], or protonation of the proximal thiolate to the inactive neutral thiol form [38]. The latter possibility is ruled out through examination of the optical spectrum of the ferrous, carbon-monoxy bound form of CYP-MP (Fig. 1A, dashed line), which displays the characteristic spectrum (λ_{max} ~ 448 nm) for thiolate ligated Fe^{2+}–CO complexes. Only minor contributions (<15%) from the catalytically inactive 'P420' form is observed. Addition of excess fatty acid (C_{12} to C_{18} chain lengths) to the ferric enzyme resulted in no detectable optical spectroscopic changes (Fig. S3), such as the low to high spin-state conversion that is readily observed in OleT and other P450s upon substrate binding [10,11].

The active-site structure of CYP-MP was further probed by X-band electron paramagnetic resonance (EPR) spectroscopy (Fig. 2). The EPR spectrum of the isolated enzyme (Fig. 2A, top trace) is comprised of one major form with g-values at 2.49, 2.26, and 1.87.

The $g_z = 2.49$ for CYP-MP is higher than those typically observed for ferric water-ligated P450s, that usually fall in the range of $g_z \leq 2.45$ [39,40]. Similarly large g_z values have been previously observed for P450s with nitrogen or anionic oxygen donors bound trans to the cysteine thiolate [36,40]. As there is no amino acid in the modeled active-site of CYP-MP (Fig. 5) that could readily provide such a ligand to the heme iron, we assign these spectroscopic features as most likely deriving from a ferric-hydroxide bound form of the enzyme. No high spin signals are observed upon the addition of any chain length fatty acid to the enzyme, in agreement with optical spectroscopic data. However, the addition of 4 M equivalents of stearic (C_{18}) acid to the enzyme results in the conversion of a fraction of the enzyme to a new low-spin ferric form with g values of 2.52, 2.26, and 1.87. This new species could in principle derive either from subtle changes in hydroxide ligand geometry, or from direct coordination of the fatty acid carboxylate to the heme. However, this latter scenario would seem unlikely based on the lack of significant optical spectroscopic changes upon fatty acid addition to CYP-MP (Fig. S3), and known structures of fatty acid bound CYP152 enzymes [10,23,25], in which the fatty acid carboxylate forms a salt bridge with a conserved active site arginine (retained as Arg256 in CYP-MP). Accordingly, the addition of shorter chain length substrates (ex. C16) which are readily metabolized by CYP-MP fails to reproduce the $g = 2.52$ signal that is specifically observed upon stearic acid binding.

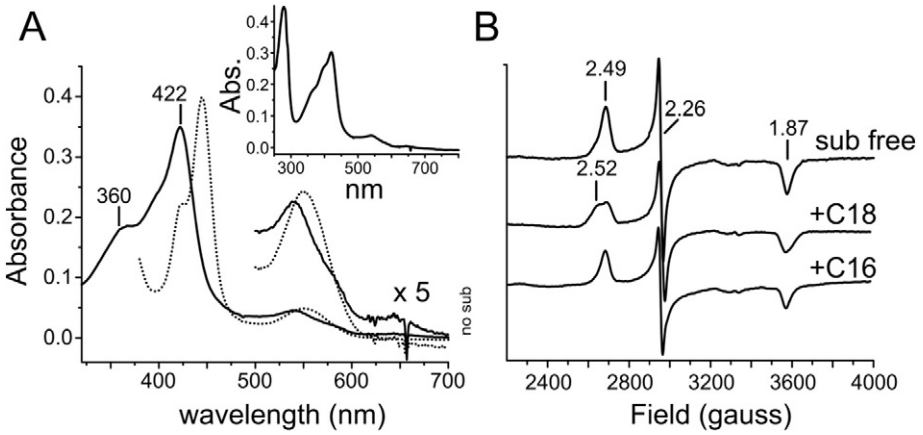

Fig. 2. UV/Vis absorption spectra of CYP-MP in ferric (solid and inset) and ferrous carbon-monoxy bound forms (A). X-band EPR of CYP-MP as purified (top trace) and upon the addition of 4 M equivalents of C18 and C16 fatty acid (middle and lower traces, respectively).

3.3. Characterization of CYP-MP reaction products

Previous multiple turnover studies of OleT have shown that the addition of excess hydrogen peroxide results in low conversion of substrate [32]. The addition of excess peroxide to CYP-MP in the presence of fatty acids resulted in similarly poor product yields (<10%) despite long incubation times, suggesting possible inactivation of the enzyme. We explored whether a slow addition of H_2O_2 would circumvent these issues in OleT, and by extension CYP-MP, enabling both higher turnover numbers and more accurate product quantitation. Assays were performed with OleT and eicosanoic acid, in which a fixed amount of oxidant (ten-fold molar excess to fatty acid), was added at varying rates, maintaining a total incubation time of 2 h. Fig. 3 demonstrates the effect of this slow H_2O_2 perfusion technique on OleT turnover yields. Nonadecene yields are maximized, and approach completion when H_2O_2 is added over a 60 min period. Nonadecene is the only product detected under these turnover conditions (Fig. S4), in accordance with single turnover studies reported earlier by our group [11].

Similar turnover methods were tested with CYP-MP and a panel of fatty acid chain length substrates. Following extraction, samples were derivatized by silylation with BSTFA to enable the detection of non-metabolized substrate (mono-), and hydroxylated (di-silylated) fatty acids, together with 1-alkene. Two internal standards, consisting of a fatty acid of similar chain length as the substrate (C_{n-2}) and hexadecane, were included to ensure accurate quantitation of all product forms. The response factors of each were determined through analysis of authentic alkene, fatty acid, and α-OH fatty acid standards.

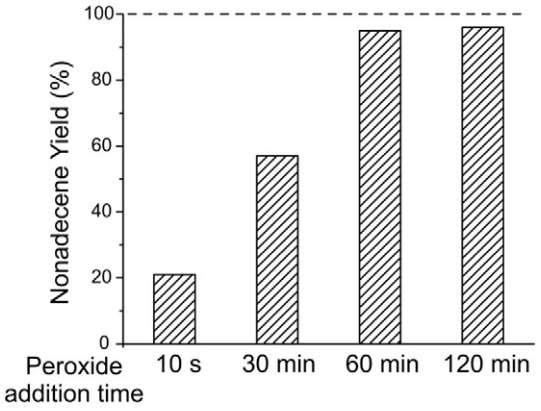

Fig. 3. Effect of varying peroxide addition time on OleT metabolism of eicosanoic acid to nonadecene. Final concentrations after mixing are 2.5 μM OleT, 250 μM fatty acid and 2.5 mM hydrogen peroxide.

Representative chromatograms for the metabolism of each substrate are included in Supplementary information (Figs. S5 to S7) and the results are summarized in Table 1. Unlike OleT, CYP-MP poorly metabolizes eicosanoic acid, and only β hydroxylated products were detected. The conversion yields considerably improve with a decrease in substrate chain length, and result in nearly stoichiometric products formed from reactions of CYP-MP and lauric acid (C_{12}). Detectable, albeit low, levels of alkene are observed in reactions of C_{18} and C_{16} substrates. As previously reported for OleT [13,32], decarboxylation chemoselectivity decreases with a reduction in carbon number, and is completely abolished in reactions of C_{14} and C_{12} substrates with CYP-MP.

Although hydroxylation at the Cβ position forms the major product across the C_{20} to C_{12} series, the turnover of short chain fatty acids, particularly C_{16} and below, results in the appearance of large distribution of products in respective chromatograms (Figs. S6 and S7). The retention times of these peaks, shortly following α and β di-silylated hydroxylated fatty acid products, suggested that they may correspond to hydroxylated derivatives that extended beyond the Cβ position. In order to unambiguously identify these putative oxidation products, GC–MS was performed. Representative mass fragmentation patterns of hydroxylated products that derive from reactions with C_{16} and C_{14} substrates are presented in Figs. 4 and S8 respectively.

The mass fragmentation patterns of the products that result from reactions of CYP-MP with C_{16} and C_{14} clearly show that γ and δ OH-fatty acids are formed. In the case of C_{14} and C_{12}, these products extend as far as the ε position, suggesting a number of substrate binding modes afforded by the CYP-MP active site. To our knowledge, these distal oxidation products have not been observed in reactions of other CYP152 enzymes, which have only been shown to form α and β fatty alcohols.

Given the relatively poor alkene formation by CYP-MP relative to OleT, we tested whether an active-site mutation may be able to rescue its activity. A noted difference from a pairwise structural comparison of OleT, BSβ, and SPα is the presence of an active-site histidine in OleT (His85) that is replaced by a glutamine in BSβ and SPα. In OleT, the His85 Nε2 group is positioned ~5.9 Å from the heme iron and could possibly serve a role to promote the decarboxylation pathway through hydrogen bonding interaction, or possible proton donation, to an incipient iron(IV)-hydroxide formed as a result of C–H bond abstraction. This position is replaced by a methionine (Met96) in CYP-MP, which is incapable of forming such a hydrogen bond. The Met96His mutant was generated, characterized by optical spectroscopy, and has similar general optical features as the wild-type enzyme in the ferric state, including a similar Soret maximum, prominent α band, and a second absorption band at 360 nm (Fig. S7). Reduction with dithionite in the presence of CO reveals that the enzyme is partially (~40%) in the inactive P420 form, observed in multiple preparations of the enzyme. The results of turnover studies with C_{12}, C_{14}, and C_{16} substrates (Table 1) show that

Table 1
Fatty acid metabolism, and product distribution profiles of WT and Met96His CYP-MP.

Cytochrome P450	Substrate	Conversion (%)	Product distributions (%)			
			1-Alkene	α-OH	β-OH	γ, δ, ε-OH
WT CYP-MP	C_{20}	<1%[a]				
	C_{18}	18.4 ± 1.2	38.3 ± 4.7	8.4 ± 5.8	48.3 ± 6.7	5.0 ± 0.8
	C_{16}	64.0 ± 4.8	23.9 ± 0.9	3.4 ± 0.1	65.4 ± 1.1	7.3 ± 0.2
	C_{14}	88. 9 ± 2.7	n.d.	3.4 ± 0.4	69.3 ± 2.6	27.3 ± 2.8
	C_{12}	99.9 ± 0.1	n.d.	7.9 ± 0.7	71.0 ± 5.5	21.1 ± 6.2
Met96His	$C_{12, 14, 16}$	<1%[b]				

n.d. not detected.
[a] Only β-hydroxylated fatty acid products were detected.
[b] Mostly β-alcohol fatty acids.

introduction of an active-site histidine does not restore alkene production. The CYP-MP Met96His mutant displays poor metabolism of fatty acids, resulting in <1% conversion. The meager levels of product that are detectable only comprise hydroxylated fatty acid products.

4. Discussion

It is shown here that CYP-MP is capable of producing alkenes, extending the unusual OleT oxidative decarboxylation reaction to a second CYP152. The observation of alcohol products, in addition to alkenes, is consistent with previous proposals that very similar chemical mechanisms give rise to both products. Production of an alkene necessitates the loss of a hydrogen from the Cβ position. Therefore, it would seem logical that the decarboxylation reaction is initiated by C–H bond abstraction by Compound I at this position. Unfortunately, the perdeuterated fatty acid probe utilized in our previous transient kinetics studies of OleT does not allow for precise targeting of this abstraction to a Cβ–H. In light of this, it is notable that Cβ alcohols are the predominant CYP-MP reaction product in reactions of all chain length (CL) substrates. C–H bond abstraction at Cβ is not the sole requirement for efficient decarboxylation. Additional structural or electronic factors are likely required to inhibit an oxygen rebound step following the formation of Compound II.

The native substrate for CYP-MP is not currently known. Given the high abundance of mono-unsaturated (largely C_{18}) fatty acids found in many *Methylobacteria* [41], it is possible that the native substrate of CYP-MP may not be among those tested in this study. Nonetheless, the spectroscopic and activity assays reported here begin to provide a more detailed framework for understanding the active site requirements for alkene formation. The capacity of CYP-MP to catalyze decarboxylation demonstrates that an active-site histidine is not an obligate requirement for substrate carbon–carbon scission. Nonetheless, CYP-MP is much less productive than OleT for the synthesis of alkenes from longer (C_{18} and C_{20}) substrates. The strict chain length dependence of CYP-MP decarboxylase activity also alludes to an importance of substrate identity in controlling the monooxygenation/decarboxylation branchpoint. For comparison, there is some ambiguity regarding the CL dependence of OleT, which may result from variations in reaction conditions, the oxidant utilized (O_2/electrons versus H_2O_2), and analytical methods employed [13,14,32]. Although reported yields vary significantly in these studies, OleT has been shown to produce increasing amounts of α and β OH-fatty acids, and consequently less alkene, upon CL reduction from C_{20} to C_{16}. An associated decreased capacity for shorter chain fatty acids to induce a low- to high-spin state conversion in OleT [10] may signal the presence of multiple substrate coordination modes within the active-site, leading to an increased accessibility of the heme iron to water. These relationships have been extensively studied in other P450s, including CYP101 mutants and substrate analogs (ex. [42–45]). While optical spin-state transitions are not directly observable for CYP-MP upon the binding of substrates, it is notable that perturbation of the ferric-hydroxide EPR spectrum is only observed upon binding of a substrate (C_{18}) that shows the largest

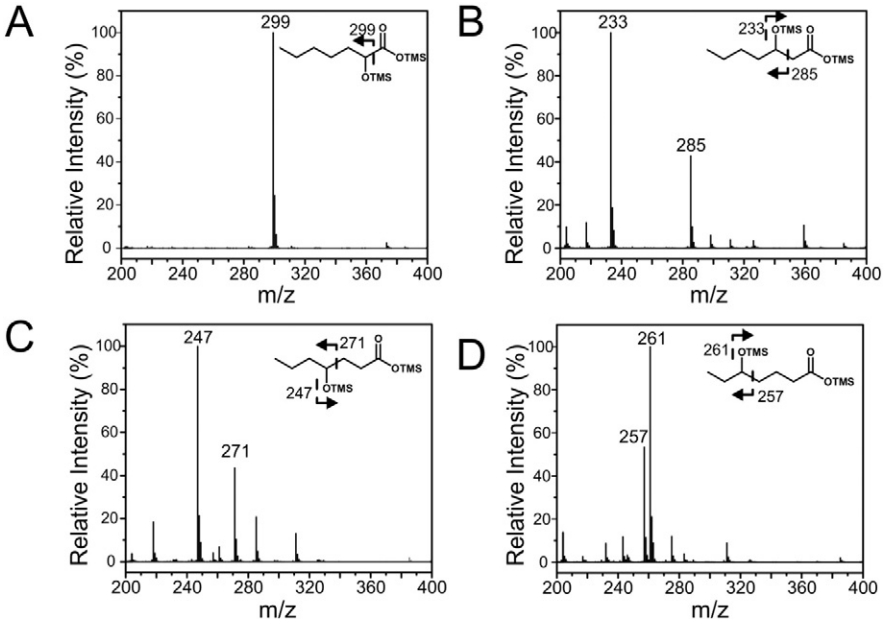

Fig. 4. GC/MS fragmentation patterns of derivatized (di-silylated) hydroxy-fatty acid products in reactions of CYP-MP, C_{16} fatty acid, and H_2O_2, showing α (A), β (B), γ (C), and δ (D) forms. The mass of major fragment ions is indicated with respective assignments in the inset.

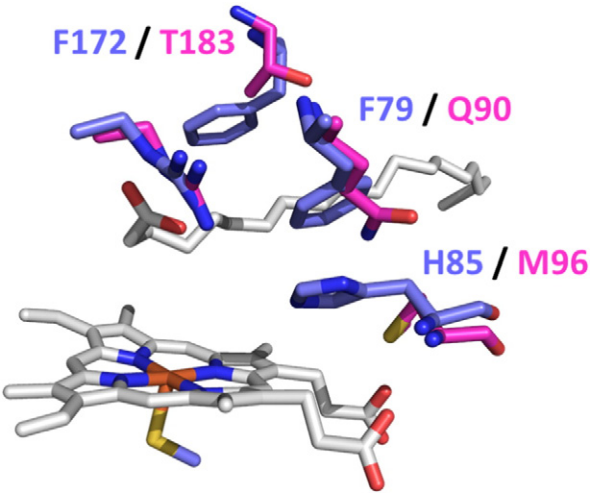

Fig. 5. Overlay of the predicted active-site structure of CYP-MP (pink) and eicosanoic acid (C_{20}) bound Ole-T (blue) PDB:4L40.

efficiency for alkene formation. Likewise, the product distributions for shorter chain fatty acids, extending as far as the Cε position for C_{12}, clearly demonstrate that shorter CL substrates adopt a variety of conformations within the CYP-MP active site. As for OleT, decreased regiospecificity compromises the efficiency of the alkene forming pathway in CYP-MP.

In order to identify the possible structural factors that may give rise to a large distribution of CYP-MP oxidation products, a homology model (based on the C_{20} fatty acid bound X-ray structure of OleT, PDB 4L40 [10]) was generated using the ITASSER server [46]. An overlay of the two active sites is shown in Fig. 5. Assuming that fatty acids bind in a similar orientation to CYP-MP as OleT, smaller hydrophilic side chains replace the phenylalanine residues found in OleT (Phe79 and 172) that lie in close contact with the substrate. Without the anchoring of these residues in CYP-MP, the fatty acid may be able to shift more readily, allowing for a greater propensity for target C–H bond abstraction and incipient oxygen rebound. Controlling substrate binding modes, in this case, may serve as a guide for understanding the differential alkene-producing ability of different CYP152 enzymes. They may also serve as a template for improving the efficiency of OleT with alternative substrates.

Acknowledgments

We thank Michael Walla for assisting with the GC–MS analysis of alkene and hydroxylated fatty acid products and Dr. John Ferry for use of a GC. This work is supported by ASPIRE grant 13020-13-33307 to T. M. M from the U.S.C. Office of the Vice President for Research.

Appendix A. Supplementary data

Supplementary data to this article can be found online at http://dx.doi.org/10.1016/j.jinorgbio.2016.02.031.

References

[1] Y. Qiu, C. Tittiger, C. Wicker-Thomas, G. Le Goff, S. Young, E. Wajnberg, T. Fricaux, N. Taquet, G.J. Blomquist, R. Feyereisen, Proc. Natl. Acad. Sci. U. S. A. 109 (2012) 14858–14863.
[2] M.A. Rude, T.S. Baron, S. Brubaker, M. Alibhai, S.B. Del Cardayre, A. Schirmer, Appl. Environ. Microbiol. 77 (2011) 1718–1727.
[3] Z. Rui, X. Li, X. Zhu, J. Liu, B. Domigan, I. Barr, J.H.D. Cate, W. Zhang, Proc. Natl. Acad. Sci. U. S. A. 111 (2014) 18237–18242.
[4] A. Schirmer, M.A. Rude, X. Li, E. Popova, S.B. del Cardayre, Science 329 (2010) 559–562.
[5] P. Kallio, A. Pasztor, K. Thiel, M.K. Akhtar, P.R. Jones, Nat. Commun. 5 (2014) 4731.
[6] B. Khara, N. Menon, C. Levy, D. Mansell, D. Das, E.N. Marsh, D. Leys, N.S. Scrutton, Chembiochem 14 (2013) 1204–1208.
[7] Y.J. Choi, S.Y. Lee, Nature 502 (2013) 571–576.
[8] M. Harger, L. Zheng, A. Moon, C. Ager, J.H. An, C. Choe, Y.L. Lai, B. Mo, D. Zong, M.D. Smith, R.G. Egbert, J.H. Mills, D. Baker, I.S. Pultz, J.B. Siegel, ACS Synth. Biol. 2 (2013) 59–62.
[9] T.P. Howard, S. Middelhaufe, K. Moore, C. Edner, D.M. Kolak, G.N. Taylor, D.A. Parker, R. Lee, N. Smirnoff, S.J. Aves, J. Love, Proc. Natl. Acad. Sci. U. S. A. 110 (2013) 7636–7641.
[10] J. Belcher, K.J. McLean, S. Matthews, L.S. Woodward, K. Fisher, S.E.J. Rigby, D.R. Nelson, D. Potts, M.T. Baynham, D.A. Parker, D. Leys, A.W. Munro, J. Biol. Chem. 289 (2014) 6535–6550.
[11] J.L. Grant, C.H. Hsieh, T.M. Makris, J. Am. Chem. Soc. 137 (2015) 4940–4943.
[12] I. Zachos, S.K. Gassmeyer, D. Bauer, V. Sieber, F. Hollmann, R. Kourist, Chem. Commun. (Cambridge, U. K.) 51 (2015) 1918–1921.
[13] A. Dennig, M. Kuhn, S. Tassoti, A. Thiessenhusen, S. Gilch, T. Bulter, T. Haas, M. Hall, K. Faber, Angew. Chem. Int. Ed. 54 (2015) 8819–8822.
[14] Y. Liu, C. Wang, J. Yan, W. Zhang, W. Guan, X. Lu, S. Li, Biotechnol. Biofuel 7 (2014) 28.
[15] T. Fujii, K. Nakamura, K. Shibuya, S. Tanase, O. Gotoh, T. Ogawa, H. Fukuda, Mol. Gen. Genet. 256 (1997) 115–120.
[16] H. Fukuda, T. Fujii, E. Sukita, M. Tazaki, S. Nagahama, T. Ogawa, Biochem. Biophys. Res. Commun. 201 (1994) 516–522.
[17] P.R.O. de Montellano, Chem. Rev. 110 (2010) 932–948.
[18] I.G. Denisov, T.M. Makris, S.G. Sligar, I. Schlichting, Chem. Rev. 105 (2005) 2253–2277.
[19] Y. Imai, I. Matsunaga, E. Kusunose, K. Ichihara, J. Biochem. 128 (2000) 189–194.
[20] I. Matsunaga, T. Sumimoto, A. Ueda, E. Kusunose, K. Ichihara, Lipids 35 (2000) 365–371.
[21] I. Matsunaga, M. Yamada, E. Kusunose, T. Miki, K. Ichihara, J. Biochem. 124 (1998) 105–110.
[22] I. Matsunaga, N. Yokotani, O. Gotoh, E. Kusunose, M. Yamada, K. Ichihara, J. Biol. Chem. 272 (1997) 23592–23596.
[23] D.S. Lee, A. Yamada, H. Sugimoto, I. Matsunaga, H. Ogura, K. Ichihara, S. Adachi, S.Y. Park, Y. Shiro, J. Biol. Chem. 278 (2003) 9761–9767.
[24] M. Girhard, S. Schuster, M. Dietrich, P. Durre, V.B. Urlacher, Biochem. Biophys. Res. Commun. 362 (2007) 114–119.
[25] T. Fujishiro, O. Shoji, S. Nagano, H. Sugimoto, Y. Shiro, Y. Watanabe, J. Biol. Chem. 286 (2011) 29941–29950.
[26] I. Matsunaga, A. Yamada, D.S. Lee, E. Obayashi, N. Fujiwara, K. Kobayashi, H. Ogura, Y. Shiro, Biochemistry 41 (2002) 1886–1892.
[27] J. Rittle, M.T. Green, Science 330 (2010) 933–937.
[28] J.T. Groves, G.A. McClusky, J. Am. Chem. Soc. 98 (1976) 859–861.
[29] J.T. Groves, G.A. McClusky, R.E. White, M.J. Coon, Biochem. Biophys. Res. Commun. 81 (1978) 154–160.
[30] D.G. Kellner, S.C. Hung, K.E. Weiss, S.G. Sligar, J. Biol. Chem. 277 (2002) 9641–9644.
[31] X. Wang, S. Peter, M. Kinne, M. Hofrichter, J.T. Groves, J. Am. Chem. Soc. 134 (2012) 12897–12900.
[32] L. Zachos, S.K. Gassmeyer, D. Bauer, V. Sieber, F. Hollmann, R. Kourist, Chem. Commun. 51 (2015) 1918–1921.
[33] P.G. Blommel, B.G. Fox, Protein Expr. Purif. 55 (2007) 53–68.
[34] E.A. Berry, B.L. Trumpower, Anal. Biochem. 161 (1987) 1–15.
[35] S. Adak, C. Crooks, Q. Wang, B.R. Crane, J.A. Tainer, E.D. Getzoff, D.J. Stuehr, J. Biol. Chem. 274 (1999) 26907–26911.
[36] N. Agmon, Chem. Phys. Lett. 244 (1995) 456–462.
[37] R.N. Austin, J.T. Groves, Metallomics 3 (2011) 775–787.
[38] P.A. Adams, J. Louw, J. Chem. Soc. Perkin Trans. 2 (1995) 1683–1690.
[39] B.J. Baas, I.G. Denisov, S.G. Sligar, Arch. Biochem. Biophys. 430 (2004) 218–228.
[40] D.P. Barr, R.P. Mason, J. Biol. Chem. 270 (1995) 12709–12716.
[41] S. Wellner, N. Lodders, P. Kampfer, Int. J. Syst. Evol. Microbiol. 62 (2012) 917–924.
[42] T.E. Carver, R.E. Brantley Jr., E.W. Singleton, R.M. Arduini, M.L. Quillin, G.N. Phillips Jr., J.S. Olson, J. Biol. Chem. 267 (1992) 14443–14450.
[43] C. Bonfils, J.L. Saldana, P. Debey, P. Maurel, C. Balny, P. Douzou, Biochimie 61 (1979) 681–687.
[44] C. Bonfils, P. Debey, P. Maurel, Biochem. Biophys. Res. Commun. 88 (1979) 1301–1307.
[45] C. Bonfils, P. Debey, P. Maurel, Biochem. Biophys. Res. Commun. 88 (1979) 1301–1307.
[46] K. Chen, L. Que Jr., J. Am. Chem. Soc. 123 (2001) 6327–6337.